Changes in tendon spatial frequency parameters with loading

Stephen J. Pearson[1], Aaron J. Engel[2], Gregory R. Bashford[2]

[1]Centre of Health, Sport and Rehabilitation Sciences Research, University of Salford, Manchester, M6 6PU, United Kingdom. [2] Dept. of Biological Systems Engineering

University of Nebraska-Lincoln, USA

Corresponding author: Dr Stephen Pearson- s.pearson@salford.ac.uk; Tel: 01612952673

Keywords: Mechanical properties, Patella Tendon, transverse strain, Ultrasound, Micro-morphology

Word count: 2000

Abstract

To examine and compare the loading related changes in micro-morphology of the patellar tendon.

Fifteen healthy young males (age 19 ± 3 yrs, body mass 83 ± 5 kg) were utilised in a within subjects matched pairs design. B mode ultrasound images were taken in the sagittal plane of the patellar tendon at rest with the knee at 90^0 flexion. Repeat images were taken whilst the subjects were carrying out maximal voluntary isometric contractions.

Spatial frequency parameters related to the tendon morphology were determined within regions of interest (ROI) from the B mode images at rest and during isometric contractions.

A number of spatial parameters were observed to be significantly different between resting and contracted images (Peak spatial frequency radius (PSFR), axis ratio, spatial Q-factor, PSFR amplitude ratio, and the sum). These spatial frequency parameters were indicative of acute alterations in the tendon micro-morphology with loading.

Acute loading modifies the micro-morphology of the tendon, as observed via spatial frequency analysis. Further research is warranted to explore its utility with regard to different loading induced micro-morphological alterations, as these could give valuable insight not only to aid strengthening of this tissue but also optimization of recovery from injury and treatment of conditions such as tendinopathies.

Introduction

Tendons are made up predominantly of collagen (60-85% of dry weight) (Józsa et al., 1989), with type I collagen being the predominant type. There are also elastin elements 1 - 2 % (Kirkendall and Garrett, 1997), which are embedded with the collagen in a proteoglycan - water matrix. These elements give tendons viscoelastic properties and as such they respond acutely to loading in a load (elastic) and time (viscous) dependent way (Ker et al., 2000).

The collagen component of the tendon can be seen to be the main structural element and its structure reflects the loading deformation characteristics seen, with a nonlinear 'toe' (beginning of loading region) region as a consequence of the 'crimp' (bunching of collagen fibres) seen in resting collagen structures (Diamant et al., 1972), to a then reasonably linear elastic region reflective of the elastin structures within the tendon and sliding of the tropocollagen molecules and associated stretching of the triple collagen helices (Folkhard et al., 1987). There is also interstitial fluid flow seen with loading of tendons, possibly representing the viscous element (Hannafin and Arnoczky, 1994). The loading of tendons can result in physiologic adaptations which may be beneficial or detrimental, dependant on the loading. Tendons **transfer** the load via mechanotransduction from the cellular matrix to the tendon cells, resulting in biochemical responses at cellular level.

Loading protocols have previously been investigated in an attempt to identify optimal strategies for adaptation and or recovery from injury and conditions such as tendinopathies. For example, a number of studies have measured tendon cross-sectional area (CSA) and observed any increases after a period of loading. Of those that have utilized MRI to determine changes it was reported that short term loading (12 weeks and 9 weeks respectively) can result in region specific hypertrophic changes (Kongsgaard et al., 2007;Seynnes et al., 2009). However other potential possibilities of adaptation are intrinsic changes to the tendon structure as indicated by increases in Young's Modulus (Reeves et al., 2003;Bohm et al., 2014). In the Bohm et al. study, high strain rate loading was seen to be preferential in producing tendon adaptation.

The mechanisms underlying adaptation are unclear. Studies examining acute cyclic loading have shown changes in transverse strain. Here reductions in the tendon thickness are evident when loaded (Wearing et al., 2013). The loading associated reduction in tendon thickness is suggested to be in part due to fluid transfer out of the tendon. However, acute changes in thickness during loading are also indicative of alterations of the tendon architecture. Here alignment and increased density of the collagen structures occurs with tensile loading (York et al., 2014). Changes in the tendon component arrangements can be indirectly described by the tendon stress/strain characteristic relationship. Below 2% strain (the toe region) represents the "stretching-out" of crimped tendon fibrils with tensile loading. This typical mechanical observation due to the 'crimped' fibril pattern can change to some degree, due to the differential crimp angle and crimp length between structures. With increased loading, a linear region in the stress strain curve appears (up to approx 4-5 % strain). Here the collagen fibrils begin to alter their conformation and align themselves in the direction of tensile loading. These characteristic alterations in the tendon micro-morphology with loading may possibly be identified with ultrasound imaging (Kostyuk et al., 2004).

Visualisation of the tendon using B-mode ultrasound shows an anisotropic speckle pattern in which the pattern or image texture and brightness depends on the spatial distribution of the acoustic scatters within the tendon. This characteristic pattern and intensity is affected by the tendon structure and alignment to the ultrasound emission waves (Kannus, 2000). For healthy tendon, the speckle pattern present has a spatial frequency signature with a significant magnitude element and narrow frequency bandwidth about the peak spatial frequency (Bashford et al., 2008).

Analysis of tendon pathology had been previously performed in the frequency domain (Bashford et al., 2008). Previous work has shown peak spatial frequency radius (PSFR) in a tendon to be correlated with tendon elasticity (Kulig et al., 2016). Tendon is made up of elastic polymers. At rest, the individual polymer are more bundled, they can be stretched a finite length before breaking (Rigby et al., 1959). If ultrasound frequency analysis is able to categorise tendon mechanical properties it may be useful to examine whether this approach is sensitive enough to detect acute alterations in the tendon micro-architecture with loading.

Thus it can be seen that the acute loading and the mode of loading may influence the tendon response with acute loading. Hence this study applies the use of spatial frequency analysis of the tendon B mode images to examine indicators of acute changes within the tendon structure.

Materials & Methods

15 male participants all gave their written informed consent and were included in this study (age 19 ± 3 yrs, body mass 83 ± 5 kg). All experimentation was approved by the local ethics committee and all procedures were in accordance with the world medical association Declaration of Helsinki (2013).

B-Mode ultrasound images (7.5 MHz 100mm linear array B-mode ultrasound probe (Mylab 70, Esaote Biomedica, Italy) with a depth setting of 30mm were taken of the patellar tendon in the sagittal plane, both whilst they were unloaded and during maximal voluntary isometric contractions (MVC), held for approx 5 secs with the knee flexed to 90^0. A familiarisation isometric contraction was performed prior to the test contraction for all subjects. Figure 1 shows an example of an unloaded and loaded tendon. For each image pair, a region of interest (ROI) was selected corresponding to the tendon tissue seen within the image. Within the ROI, Cohens d was calculated by

$$d = \frac{\bar{X}}{\sigma_X} \qquad 1$$

where X is the paired differences of the samples and σ_X is the standard deviation of the paired differences. P-values were estimated using a permutation test on X. A total of 10000 permutations were used.

$$p = \frac{\sum_{n=1}^{10000}(\overline{X_n} \geq \overline{X_0})}{10000} \qquad 2$$

Here $\overline{X_0}$ is the observed average difference and X_n is the n-th permutation of the observed data.

Image analysis and parameter extraction

Spatial frequency analysis was carried out in a manner similar to Bashford and co workers 2008 (Bashford et al., 2008). Briefly, digitally stored images in jpeg format were imported into MATLAB where all analyses were completed with custom in-house algorithms. An ROI enclosing the tendon area of interest was selected by cursor (See Fig 1). Within the ROI, every possible 2mm-square kernel circumscribed by the ROI was analyzed. For each kernel, eight spatial frequency parameters were extracted (see Table 1). The number of kernels circumscribed by the ROI was the number of observations made of each parameter.

Statistical analyses

All statistical analyses were carried out in SPSS (Ver 20; IBM Corp) and MATLAB (ver 8.4, Mathworks, Natick, MA). SPSS was used to calculate normality of data and determined by the Shapiro Wilks test. Paired Student t-tests were utilised to determine any significant differences for tendon thickness and between the frequency determinants for the ROI. Alpha level was set to 0.05.

MATLAB was used to analyze spatial frequency parameter statistics. Paired student t-tests were utilized to determine any significant differences between the spatial frequency parameters between loaded and unloaded tendons. The alpha level was set to 0.05.

Results

Table 2 shows the paired statistics for unloaded to loaded tendons. Here only the whole tendon data is shown. The parameters that met statistically significant differences are the Peak Spatial Frequency Radius, Axis Ratio, Mmax%, and the Sum where tendon loading produced an increase of 0.51, 0.67, 1.21 and decrease of 1.04 standard deviations of the estimate respectively.

Discussion

The results here show characteristic changes in the frequency analysis of the patellar tendon during acute maximal isometric loading. In particular, increases in the peak spatial frequency radius, axis ratio, and sum were seen with a concurrent decrease in normalized peak spatial frequency amplitude (Mmax%) . To understand the change of PSFR, Axis Ratio, Mmax%, and the Sum (local intensity), it is necessary to understand the natural structure of the tendon. Tendons are viscoelastic in nature due to the composite elements (elastin/collagen and the proteoglycan water matrix). This viscoelastic characteristic results in creep whereby elongation increases with a fixed load application, and stress relaxation whereby the stress is reduced with a fixed elongation (Clatworthy et al., 1999; Ker et al., 2000). If the elongation is determined during application of force it can be seen to be a curvilinear relationship. Here larger elongation is seen initially, probably due to the uncrimping of the collagen fibrils in the direction of the applied stress and the beginning of increased lateral packing of the fibrils (Diamant et al., 1972;Kirkendall and Garrett, 1997;Misof et al., 1997). After this initial elongation there appears a quite linear portion, reflective of the stretching and further alignment of the collagen helices and sliding of the tropocollagen molecules (Folkhard et al., 1987). These alterations in the tendon structure during loading can explain an increase in the Peak Spatial Frequency Radius which is expected as the collagen fibres straighten and move slightly closer together. This same process is responsible for the increase in the Axis Ratio, but here it is predominantly influenced by the fibre straightening.

The increase in the sum measure may be reflective of alterations in the water content of the tendon. It is well known that an inflamed tendon or muscle will have higher water content and will show up darker on a B-Mode ultrasound scan. This is because water will decrease the scatterer density. Thus during loading it may be that water or fluid is displaced temporarily through the intracellular spaces out of the tendon (Hannafin and Arnoczky, 1994;Lanir et al., 1988), along with increased density/alignment of the collagen fibrils, resulting in a brighter image signature and hence increased sum value. Although it must be stated that the likelihood of the suggested exchange of fluid between the interstitial spaces is currently unknown during short term contractions such as here and is in need of further investigation.

In addition to the loaded tendon possibly increasing the overall density of the scatterers and hence the observed increased brightness, the brighter speckle pattern is proposed based on the understanding of its statistics. Initially, in a relaxed state the tendon extracellular matrix (ECM) is bundled with random orientations, upon elongation the random kinks in the ECM become smoother and their scattering will be coherent with the nearby ECM scattering. The probability density function for the speckle pattern of the tendon, which is already a Rician distribution, becomes a stronger Rician distribution moving further away from the standard Rayleigh distribution which defines the speckle pattern of unstructured tissue. This explanation for the increase in speckle pattern brightness agrees with the explanation showing an increase of the Peak Spatial Frequency and the Axis Ratio.

Tendons that are routinely 'loaded' become stiffer and show intrinsic modifications indicative of the strengthening of the tendon as it adapts to the loads experienced (Wiesinger et al., 2015)**.** Previous work has indicated these increases in stiffness with exercise (Onambélé et al., 2008;Burgess et al., 2009). In contrast, unloading can be seen to result in decrease in the tendon mechanical properties (de Boer et al., 2007). Recently it has been shown that the tendon mechanical properties are related to the spectral frequencies in the ultrasound image of degenerative tendons (Kulig et al., 2016). Here it was stated that the peak spatial frequency radius showed a good relationship with the determined stiffness of the Achilles tendon (r = 0.74). This relationship was not seen in healthy tendons however. It was not clear from the study if the spatial parameters were determined with the tendon at rest or during loading. This may be of importance as healthy tendon may not react the same to loading as degenerative tendon and if spectral parameters had been determined both at rest and during loading, perhaps more insight could have been gained into the differences. Indeed here we show in healthy tendons using the same approach, qualitative changes when going from unloaded to loaded as identified by the spectral parameters. This approach could yield interesting information regarding the tendon adaptability to both acute and chronic loading protocols. The ability to monitor tendon in this way may enable an index of healthy tendon to be established, which may be able to detect when a tendon is beginning to maladapt. Whilst we acknowledge that more work needs to be done to further validate this method i.e. repeatability of measures and examination of the sensitivity under a variety of conditions to determine its viability and limitations.

The potential information from this technique would allow changes to the training programme to be made for instance in the case of an athlete. Where rehabilitation was being carried out it may give valuable insight into the significance or effectiveness of the rehabilitation programme enabling optimisation of the rehabilitation on an individual level.

Acknowledgements: No sources of funding are associated with this work. To the authors knowledge there are no conflicts of interest.

References

Bashford, G.R., Tomsen, N., Arya, S., Burnfield, J.M., Kulig, K., 2008. Tendinopathy discrimination by use of spatial frequency parameters in ultrasound b-mode images. IEEE Trans. Med. Imaging 27, 608–615. doi:10.1109/TMI.2007.912389

Bohm, S., Mersmann, F., Tettke, M., Kraft, M., Arampatzis, A., 2014. Human Achilles tendon plasticity in response to cyclic strain: effect of rate and duration. J. Exp. Biol. 217, 4010–7. doi:10.1242/jeb.112268

Burgess, K.E., Graham-Smith, P., Pearson, S.J., 2009. Effect of acute tensile loading on gender-specific tendon structural and mechanical properties. J. Orthop. Res. 27, 510–6. doi:10.1002/jor.20768

Clatworthy, M.G., Annear, P., Bulow, J.U., Bartlett, R.J., 1999. Tunnel widening in anterior cruciate ligament reconstruction: a prospective evaluation of hamstring and patella tendon grafts. Knee Surg. Sports Traumatol. Arthrosc. 7, 138–45. doi:10.1007/s001670050138

de Boer, M.D., Maganaris, C.N., Seynnes, O.R., Rennie, M.J., Narici, M. V, 2007. Time course of muscular, neural and tendinous adaptations to 23 day unilateral lower-limb suspension in young men. J. Physiol. 583, 1079–91. doi:10.1113/jphysiol.2007.135392

Diamant, J., Keller, A., Baer, E., Litt, M., Arridge, R.G., 1972. Collagen; ultrastructure and its relation to mechanical properties as a function of ageing. Proc. R. Soc. London. Ser. B, Biol. Sci. 180, 293–315.

Folkhard, W., Christmann, D., Geercken, W., Knörzer, E., Koch, M.H., Mosler, E., Nemetschek-Gansler, H., Nemetschek, T., 1987. Twisted fibrils are a structural principle in the assembly of interstitial collagens, chordae tendineae included. Zeitschrift für Naturforschung. C, J. Biosci. 42, 1303–6.

Hannafin, J.A., Arnoczky, S.P., 1994. Effect of cyclic and static tensile loading on water content and solute diffusion in canine flexor tendons: an in vitro study. J. Orthop. Res. 12, 350–6.

doi:10.1002/jor.1100120307

Józsa, L., Lehto, M., Kvist, M., Bálint, J.B., Reffy, A., 1989. Alterations in dry mass content of collagen fibers in degenerative tendinopathy and tendon-rupture. Matrix 9, 140–6.

Kannus, P., 2000. Structure of the tendon connective tissue. Scand. J. Med. Sci. Sports 10, 312–20.

Ker, R.F., Wang, X.T., Pike, A. V, 2000. Fatigue quality of mammalian tendons. J. Exp. Biol. 203, 1317–27.

Kirkendall, D.T., Garrett, W.E., 1997. Function and biomechanics of tendons. Scand. J. Med. Sci. Sports 7, 62–6.

Kongsgaard, M., Reitelseder, S., Pedersen, T.G., Holm, L., Aagaard, P., Kjaer, M., Magnusson, S.P., 2007. Region specific patellar tendon hypertrophy in humans following resistance training. Acta Physiol. (Oxf). 191, 111–21. doi:10.1111/j.1748-1716.2007.01714.x

Kostyuk, O., Birch, H.L., Mudera, V., Brown, R.A., 2004. Structural changes in loaded equine tendons can be monitored by a novel spectroscopic technique. J. Physiol. 554, 791–801. doi:10.1113/jphysiol.2003.054809

Kulig, K., Chang, Y.-J., Winiarski, S., Bashford, G.R., 2016. ULTRASOUND-BASED TENDON MICROMORPHOLOGY PREDICTS MECHANICAL CHARACTERISTICS OF DEGENERATED TENDONS. Ultrasound Med. Biol. 42, 664–673. doi:10.1016/j.ultrasmedbio.2015.11.013

Lanir, Y., Salant, E.L., Foux, A., 1988. Physico-chemical and microstructural changes in collagen fiber bundles following stretch in-vitro. Biorheology 25, 591–603.

Misof, k, Rapp, G., Fratzl, P., 1997. A new molecular model for collagen elasticity based on synchrotron X-ray scattering evidence. Biophys J 72, 1376–81.

Onambélé, G., Maganaris, C., Mian, O., Tam, E., Rejc, E., McEwan, I., Narici, M., 2008. Neuromuscular and balance responses to flywheel inertial versus weight training in older persons. - PubMed - NCBI. J Biomech 41, 3133–8.

Reeves, N.D., Maganaris, C.N., Narici, M. V, 2003. Effect of strength training on human patella tendon mechanical properties of older individuals. J. Physiol. 548, 971–81. doi:10.1113/jphysiol.2002.035576

Rigby, B.J., Hirai, N., Spikes, J.D., Eyring, H., 1959. The Mechanical Properties of Rat Tail Tendon. J. Gen. Physiol. 43, 265–83. doi:10.1016/j.jsb.2011.07.013

Seynnes, O.R., Erskine, R.M., Maganaris, C.N., Longo, S., Simoneau, E.M., Grosset, J.F., Narici, M. V, 2009. Training-induced changes in structural and mechanical properties of the patellar tendon are related to muscle hypertrophy but not to strength gains. J. Appl. Physiol. 107, 523–30. doi:10.1152/japplphysiol.00213.2009

Tuthill, T., Rubin, J., Fowlkes, J., Jamadar, D., Bude, R., 1999. Frequency analysis of echo texture in tendon. - PubMed - NCBI. Ultrasound Med Biol 25, 959–68.

Wearing, S.C., Hooper, S.L., Purdam, C., Cook, J., Grigg, N., Locke, S., Smeathers, J.E., 2013. The acute transverse strain response of the patellar tendon to quadriceps exercise. Med. Sci. Sports Exerc. 45, 772–777. doi:10.1249/MSS.0b013e318279a81a

Wiesinger, H.-P., Kösters, A., Müller, E., Seynnes, O.R., 2015. Effects of Increased Loading on In Vivo Tendon Properties: A Systematic Review. Med. Sci. Sports Exerc. 47, 1885–95. doi:10.1249/MSS.0000000000000603

York, T., Kahan, L., Lake, S.P., Gruev, V., 2014. Real-time high-resolution measurement of collagen alignment in dynamically loaded soft tissue. J. Biomed. Opt. 19, 66011.

doi:10.1117/1.JBO.19.6.066011

Figure caption

Figure 1. Typical saggital plane ultrasound image of the patellar tendon showing the enclosed ROI rectangle box in green overlaying the patellar tendon.

Figures

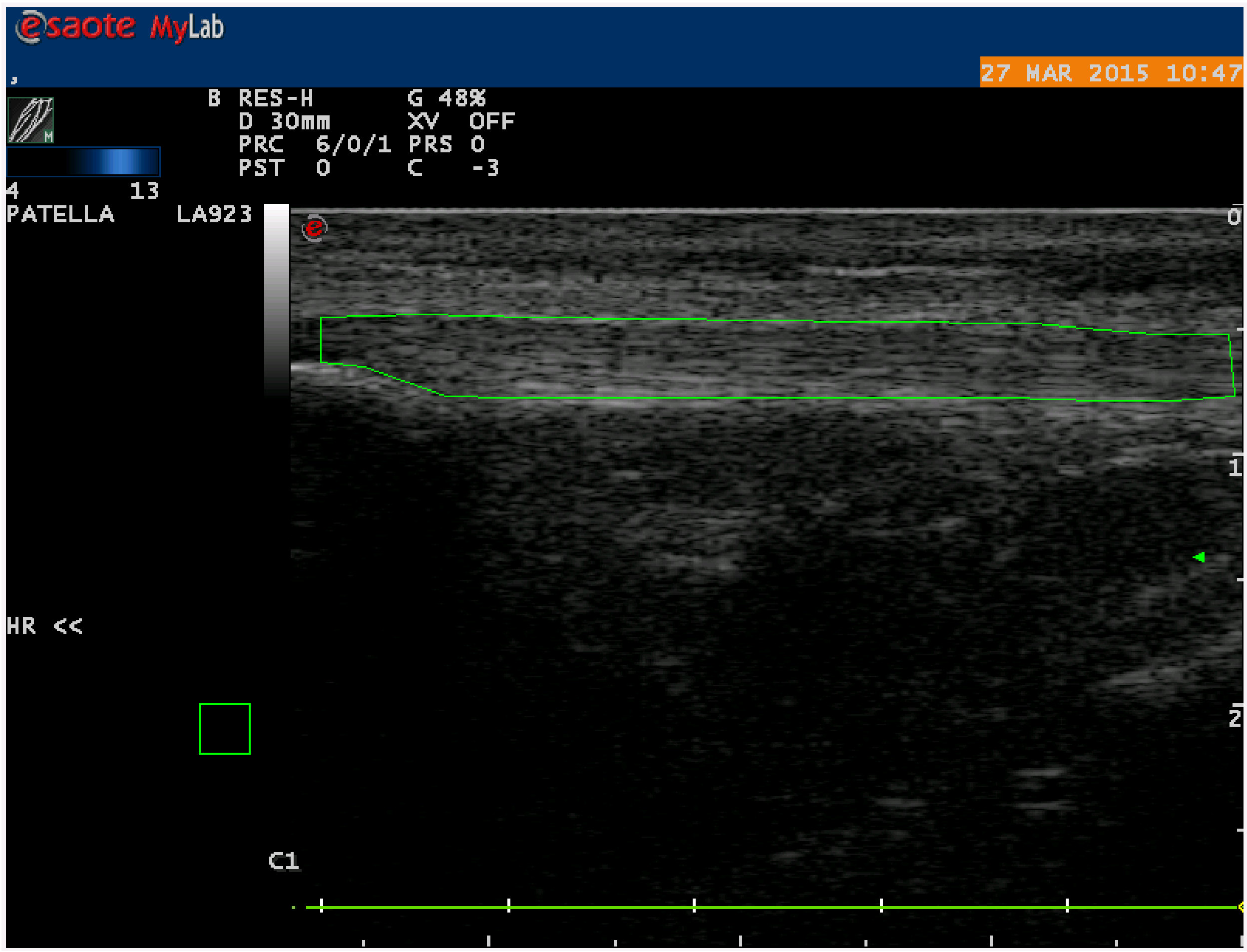
esaote MyLab
27 MAR 2015 10:47
B RES-H
D 30mm
PRC 6/0/1
PST 0
G 48%
XV OFF
PRS 0
C -3
4 13
PATELLA LA923
0
1
2
HR <<
C1

Tables

Table 1. Spatial frequency parameters analysed for the tendon images and descriptions

Table 1.		
Parameter #	**Parameter Name**	**Description/tissue characteristic indicators**
1	Peak Spatial Frequency	Distance from origin to spatial frequency peak of greatest amplitude on 2-D FFT spectrum The purity of fibre alignment modulated by the axial resolution of the scanner
2	P6 Width	Average of horizontal and vertical -6 dB widths of greatest amplitude spatial frequency peak on 2-D FFT spectrum Decreasing P6 indicates less obtuse angular entanglement between tendon fibres
3	Q6 Factor	Ratio of Peak Spatial Frequency to P6 Width A normalization factor to facilitate comparison of fibre packing with fibre alignment
4	Mmax	Value of the maximum point of amplitude on 2-D FFT The strength of the most prominent fibre spacing of the

		tendon
5	Mmax Percent	Ratio of Mmax to the total intensity of pixels in the 2-D FFT A comparison of fibres that are highly aligned with those aligned randomly
6	Sum	Sum of intensities of original image kernel pixels Overall brightness of the image
7	Axis Ratio*	Major-to-minor axis ratio of ellipsoidal fit 16 X 16 center pixel region of 2-D FFT Comparing the elongation of spatial frequencies in orthogonal directions – the higher this number, the more anisotropic the elongation is, indicating uniform alignment across the ROI
8	Ellipse Rotation*	Rotation from vertical axis of ellipsoid fit to 2-D FFT The angle between the transducer axis and the most prominent alignment of tendon fibres
* indicates parameter used by Tuthill ((Tuthill et al., 1999))		

Table 2. The paired statistics for unloaded to loaded tendons. Unloaded and Loaded data are mean values. Parameters for which a significant change were observed are the Peak Spatial Frequency Radius, Axis Ratio, Mmax%, and the Sum (shown in bold).

Whole Tendon (Paired Stats)

			unloaded to loaded	
	Unloaded	Loaded	Cohen's d	p-value
Peak Spatial Frequency Radius	2.195	2.282	**0.51**	**0.03**
P6	0.640	0.639	-0.04	0.43
Q6	28.05	29.26	0.50	0.04
MMax	1458	1455	-0.08	0.38
M-Max_%	2.456	2.153	**-1.04**	**0.0006**
Axis Ratio	4.269	4.494	**0.67**	**0.01**
Ellipse Rotation	89.81	89.85	0.26	0.17
Sum	60425	67841	**1.21**	**0.0002**